

Observation of Nonlinear Frequency-Sweeping Suppression with rf Diffusion

D. Maslovsky,* B. Levitt, and M. E. Mauel

Department of Applied Physics and Applied Mathematics, Columbia University, New York, New York 10027

(Received 6 November 2002; published 7 May 2003)

Nonlinear frequency sweeping of unstable waves in a laboratory plasma is suppressed upon application of rf fields. Frequency sweeping is driven by a population of energetic electrons trapped in a magnetic dipole field that excite drift-resonant potential fluctuations and create coherent structures in phase space. Self-consistent numerical simulation reproduces the suppression and suggests an explanation due to rf scattering of energetic electrons that destroys the phase-space structures.

DOI: 10.1103/PhysRevLett.90.185001

PACS numbers: 52.35.Mw, 52.72.+v, 94.30.Hn

Resonant interactions between waves and particles are among the most important and interesting dynamical processes occurring within collisionless plasma. Resonant particles exchange energy with the wave fields, and, as a consequence, their dynamics can lead to phase-space mixing [1,2], trapping [3], and persistent phase-space structures within turbulence [4,5]. Recently, Berk and co-workers [6] have described spontaneous frequency sweeping occurring after a period of explosive growth in resonant particle instabilities near threshold [7,8]. Frequency sweeping is associated with the formation of hole-clump pairs that evolve in the particle phase space and support nonlinear waves with time-varying frequencies. Both the waves and the phase-space structures can have lifetimes long compared to resonant trapping times provided the competing rate of stochastic velocity-space diffusion, characterized by the parameter ν_{eff} , is small compared to the growth rate, γ .

In this Letter, we report the first observation of the suppression of nonlinear frequency sweeping by the controlled application of low-power rf fields. The observations were made in the Collisionless Terrella Experiment (CTX) [9,10], where spontaneous frequency sweeping occurs during the nonlinear evolution of the hot electron interchange (HEI) instability [11–13]. The HEI instability creates intense electrostatic potential perturbations that propagate in the direction of the magnetic drifts of energetic trapped electrons. Those electrons that resonate with the propagating potential can move radially across surfaces of constant magnetic flux, ψ , until they detune from resonance. Because the magnetic drift frequency, ω_d , scales both linearly with particle energy and in radius as $\psi^2 \propto 1/R^2$, complex phase-space structures appear in the combined energy and particle phase spaces [14]. When we apply rf fields that resonate with electron cyclotron motion at specific locations, frequency sweeping stops only to reappear abruptly when the rf fields are switched off.

A self-consistent nonlinear simulation, used to interpret the observations, successfully reproduces both the global mode structures and the rising tones of the observed potential fluctuations [13]. When spatially local-

ized energy diffusion is introduced into the simulation, the observed frequency sweeping stops because the bounced-averaged quasilinear diffusion due to the rf fields destroys the phase-space structures. The energy diffusion corresponds to the quasilinear diffusion expected for low-power electron cyclotron resonance heating (ECRH) [15], and it is analogous to the velocity-space diffusion, proportional to ν_{eff}^3 defined by Berk and co-workers [6].

The observations reported here are related to previous observations of mode frequency splitting and chaotic dynamics of Alfvén eigenmodes driven by fast ions trapped in a tokamak [16–18]. In these earlier experiments, a population of energetic protons created by ion cyclotron resonance heating (ICRH), resonated with amplified toroidal Alfvén eigenmodes. The wave-particle resonances occupied narrow regions in particle phase space and the global mode structures were spatially localized. At sufficiently high ICRH power levels ($P > 4$ MW) and by specially preparing the plasma current profiles, the mode amplitude was modulated and the mode spectrum was broadened in a manner predicted by the general nonlinear model for resonant wave-particle instability near threshold [8]. The behavior of the saturated instability could be characterized by the ratio of the eigenmode growth rate, γ , and the rate of stochastic velocity-space diffusion, ν_{eff} . When ν_{eff}/γ decreased to ~ 2.1 , nonlinear sidebands appeared [16]. When $\nu_{\text{eff}}/\gamma < 2.0$, the instability spectrum became broadband rather than discrete [18]. Although much higher ICRH power ($P > 10$ MW) was applied, the strongly nonlinear regime characterized with frequency sweeping and $\nu_{\text{eff}}/\gamma < 1$ was not observed. It was believed that increasing ICRH power increased both the eigenmode growth rate, γ , and the rf scattering rate, ν_{eff} , in proportion.

In contrast with these other observations, frequency sweeping is characteristic of the nonlinear saturation of the HEI instability in the CTX device. The HEI instability has a high growth rate, $\gamma \sim 0.1\omega_d$, saturates with large amplitudes, $\Phi > 100$ V, and exhibits collisionless wave-particle resonances, $\nu_{\text{eff}} \rightarrow 0$. Previous reports have described the complex, time evolution of the

HEI frequency spectrum as well as (i) the use of ECRH to create plasma confined by a strong magnetic dipole, (ii) the structure of the unstable eigenmodes, and (iii) the effect of the resonant electrostatic potential fluctuations on energetic electron radial transport [9,10,12,13,19]. Reference [12] interpreted the strong modulations of energetic electron flux reported in Refs. [9,10] as a consequence of phase-space structures.

Figure 1 shows a schematic of the CTX device. The HEI instability is excited by a non-Maxwellian population of energetic electrons (1–60 keV) produced with injection of approximately 1 kW of 2.45 GHz microwave power. The ECR heating and energetic electron production rate are known to be spatially localized near the fundamental cyclotron resonance at the dipole's equator. Typically, the microwave heating pulses last about 0.7 s, and the energetic electron pressure is adjusted by changing the background hydrogen gas pressure ($\sim 10^{-4}$ Pa). The microwave discharge created from ECR heating is followed by an “afterglow” that begins when the primary microwave heating is switched off and ends more than 0.1 s later as the energetic electrons are lost to the poles. Whenever the energetic electrons are sufficiently intense, strong, quasiperiodic bursts of HEI instability occur during the ECR heating phase followed by a much longer period of continuous HEI instability during the afterglow. Frequency sweeping occurs at both times, and the rate of frequency sweeping is faster when the energetic electron population is more intense.

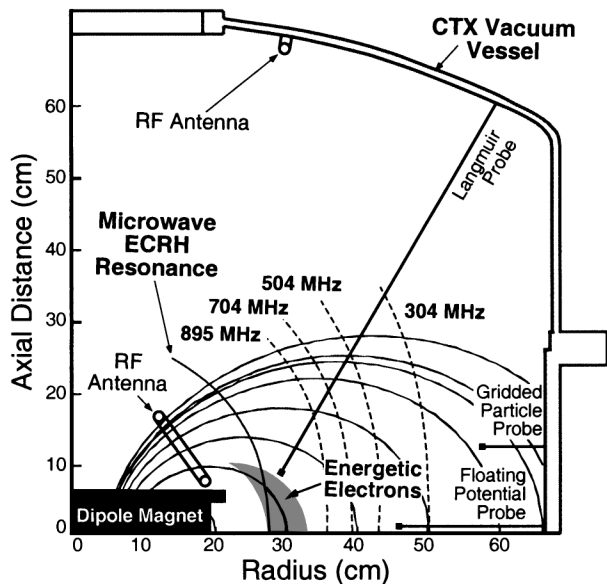


FIG. 1. A quadrant view of the cross section of the CTX device showing the magnetic field topology and the locations of the resonant cyclotron frequencies applied in these experiments. Also shown are the approximate location of the energetic trapped electrons created by high-power ECRH heating, the rf antenna locations, and some probe diagnostics.

Frequency sweeping is suppressed when rf fields are excited at low power by magnetostatic antennas placed within the vacuum chamber. We use the antennas to excite low-order cavity modes of the vacuum vessel at particular frequencies such as 304, 504, 704, and 895 MHz. Figure 1 shows two locations for this antenna: either near a pole of the dipole magnet or at the outer vacuum chamber wall. Both antennas produce equivalent frequency sweeping suppression.

Figure 2 shows a typical case of frequency sweeping suppression during the afterglow phase of the discharge. During the afterglow, microwave ECR heating is switched off. Phase-space diffusion governed by electron pitch-angle scattering essentially vanishes, $\nu_{\text{eff}} \sim 10^{-6}\omega_d$. Frequency sweeping extends to high frequency ($f > 10$ MHz) and persists for long times. When low-power rf is applied ($P \approx 50$ W, and much less than the 1 kW heating power), frequency sweeping stops until the rf fields are switched off. At lower power levels ($P \approx 20$ W), the higher azimuthal modes ($m = 2, 3$) are suppressed before suppression of the low azimuthal modes ($m = 1$), and the rate of frequency sweeping decreases just prior to suppression. The low-power levels applied (a few percent of the ECR heating power) and the

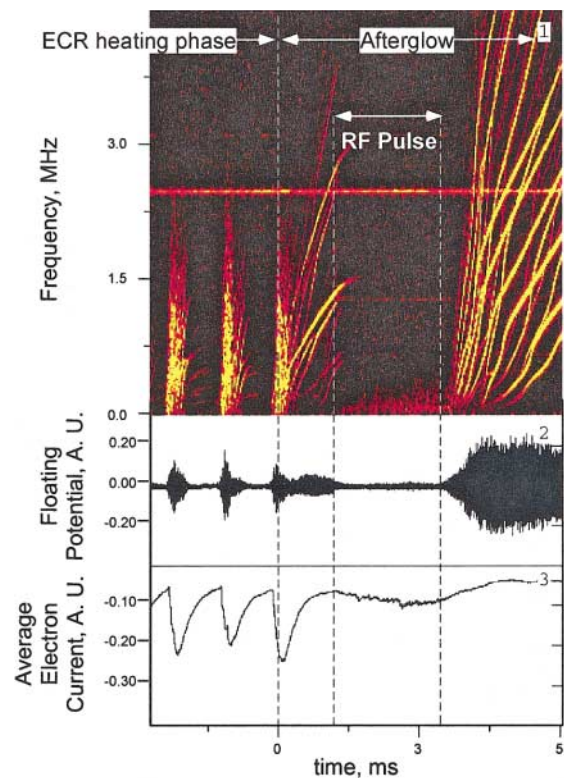


FIG. 2 (color). An example of the suppression of frequency sweeping during the “afterglow” caused by a pulse of 701.3 MHz, 34 W rf fields. From top to bottom, the plot shows (1) time-frequency spectrogram, (2) floating potential fluctuations, (3) time-averaged hot electron current to gridded particle analyzer located at 57 cm.

reappearance of nonlinear frequency sweeping at the end of the rf pulse implies that applied rf fields do not directly create global changes in electron distribution. Instead, we believe the rf fields cause ν_{eff} to increase within a localized radial region that corresponds to fundamental cyclotron resonance with the applied rf fields.

During high-power microwave heating, the HEI instability appears in quasiperiodic bursts and the frequency spectrum of each burst is complex. Frequency sweeping occurs only after a period of broadbanded instability and reaches a maximum frequency that is lower than seen during the afterglow. We find frequency sweeping is also suppressed during the microwave heating phase whenever equivalent rf fields are applied. Figure 3 summarizes the power levels measured during the heating phase that lead to frequency sweeping suppression. The intensity of fluctuations, within a frequency band $1.9 \text{ MHz} \leq f \leq 2.1 \text{ MHz}$, is normalized to the intensity below that band and plotted as a function of applied rf power. Error bars result from discharge-to-discharge variability. This provides a convenient measure of frequency sweeping during the 300–500 μs quasiperiodic instability bursts.

The presence of frequency sweeping during the ECR heating phase requires explanation—especially since ECR fields at much lower power levels are seen to suppress frequency sweeping. During the ECR heating phase, the spectral content of the HEI instability bursts evolves in time. (See Ref. [10], especially Fig. 5.) Initially, the frequency spectrum of the HEI is broadbanded and chaotic. Wave-particle resonances are closely spaced in phase space, and this induces global chaos. The energetic electrons (heated by the 2.45 GHz microwaves and localized near the equatorial position where $B = 875 \text{ G}$) are expelled radially by the HEI bursts while preserving μ and

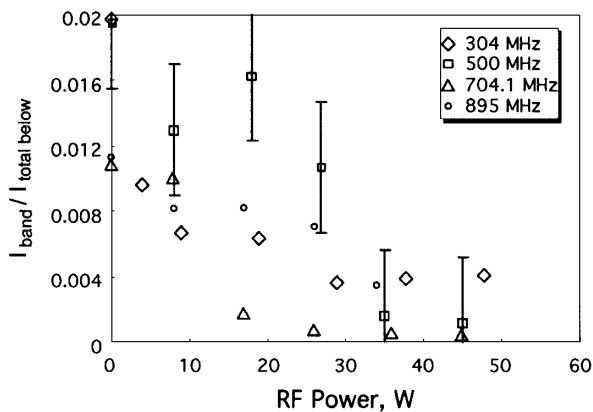


FIG. 3. Frequency sweeping suppression during ECR heating phase for four representative frequencies of applied rf fields is illustrated by the frequency sweeping amount, $I_{\text{band}}/I_{\text{total below}}$, as a function of power of applied rf field. Here, I_{band} is the intensity of measured fluctuations inside the frequency band $1.9 \text{ MHz} \leq f \leq 2.1 \text{ MHz}$, and $I_{\text{total below}}$ is the total intensity below the upper limit of the frequency band $f < 2.1 \text{ MHz}$.

J [19,20]. As the electrons move outward, no further cyclotron resonance is possible because of the magnetic mirror effect. The collisionless, outward radial transport therefore creates an energetic electron “disk” at the dipole’s equator that limits resonance with the 2.45 GHz microwaves. Frequency sweeping is only observed *after* the outward expansion of the energetic electrons when the radially broadened energetic electron disk can support phase-space “holes” that do not experience rf scattering from the $B = 875 \text{ G}$ cyclotron resonance.

We have modified a nonlinear, self-consistent numerical simulation in order to interpret the observed frequency sweeping suppression. This simulation explicitly solves for the evolution of cold ion and energetic electron number densities and the electrostatic potential, Φ , on the (ψ, φ) plane. (ψ, φ) are simultaneously the canonical coordinates of the electrons’ guiding-center drift Hamiltonian (i.e., the electron phase space) and the magnetic coordinates of the dipole, $\mathbf{B} = \nabla\psi \times \nabla\varphi$ [21]. Plasma $\mathbf{E} \times \mathbf{B}$ drifts, ion polarization drifts, and energetic electron magnetic drifts determine particle dynamics, and Poisson’s equation in magnetic coordinates determines the nonlinear evolution of the potential.

Cyclotron resonance due to the applied microwave and rf fields is modeled as causing diffusion of energetic electrons in μ space according to

$$\frac{\partial}{\partial t} F(\mu, \psi, \varphi, t) = D(\psi, t) \frac{\partial^2}{\partial \mu^2} (F - F^*), \quad (1)$$

where D is the magnitude of simulated diffusion, and $F^*(\mu)$ is a reference distribution function that is defined so that ECR diffusion leaves unchanged the initial electron energy distribution while redistributing electrons on any flux tube containing phase-space holes. The magnitude of diffusion is related to the effective collisionality specified in Berk’s formulation (Ref. [6], Eq. 14) by $\nu_{\text{eff}}^3 = 9D(\psi)(cB/e\psi)^2$; however, ν_{eff} is not uniform across phase space in our model. To simplify comparison with Ref. [6], we define $\langle \nu_{\text{eff}} \rangle$ to be the flux average of $\nu_{\text{eff}}(\psi)$. The radial variation of $D(\psi)$ depends upon the frequency of the applied microwave or rf fields. We model $D(\psi)$ to be largest at the equatorial cyclotron resonance and to vanish for flux surfaces differing by factors exceeding $\pm 10\%$ to $\pm 25\%$. By modeling the initial radial profile of the trapped electrons to represent (within experimental uncertainties) measurements, the only adjustable parameters in the model are the form of $D(\psi)$ and a constant, nonresonant dissipation that gradually damps the potential at a rate γ_d .

Figure 4 shows two examples of simulated frequency sweeping suppression. The nonresonant damping, γ_d , was adjusted, so that $\gamma_L/\gamma_d = 1.6$. As the magnitude of diffusion is increased, $F(\mu, \psi, \varphi)$ is redistributed along μ , and the ratio $\langle \nu_{\text{eff}}/\gamma \rangle$ is changed from $\langle \nu_{\text{eff}}/\gamma \rangle = 0.45$ [Fig. 4(A)] to $\langle \nu_{\text{eff}}/\gamma \rangle = 1.7$ [Fig. 4(B)]. The frequency

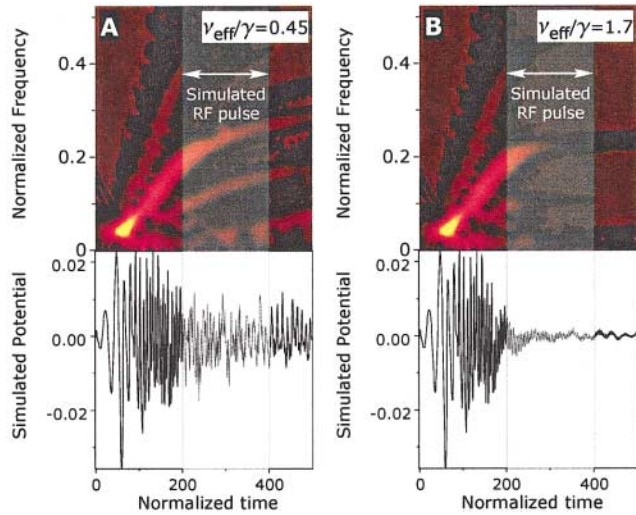


FIG. 4 (color). Numerical simulation of frequency sweeping suppression. Two cases with $\gamma_L/\gamma_d = 1.6$ shown: (A) $\langle \nu_{\text{eff}} \rangle / \gamma = 0.45$; (B) $\langle \nu_{\text{eff}} \rangle / \gamma = 1.7$. In both cases, simulated diffusion is applied from $t = 200$ to $t = 400$ in normalized time units.

sweeping is suppressed in a way similar to that observed experimentally. This coincides with the destruction of the phase-space holes required as part of the process of coherent frequency sweeping. The presence or absence of frequency sweeping is in agreement with criteria defined by Berk [6]. In particular, (i) the system must be near the linear instability threshold, $\gamma_L < 2.5\gamma_d$, and (ii) collisional effects need to be sufficiently weak to allow the explosive initiation of holes and clumps, $\langle \nu_{\text{eff}} / \gamma \rangle \leq 1$.

The rate of rf diffusion, D , required in the simulation to suppress frequency sweeping is comparable to the diffusion induced by the applied rf fields. When Eq. (1) is integrated over particle energy, $\mu B(\psi)$, and plasma volume, the power required to suppress the frequency sweeping in Fig. 4(B) is found to be ~ 50 W with reasonable estimates of electron profiles and $-\int d\mu \partial / \partial \mu (F - F^*) \leq N_h / 2\mu_0$. We find it significant that the simulated rf diffusion induced by the 2.45 GHz microwaves at a 1 kW level does not suppress frequency sweeping when $D(\psi)$ is localized at the peak electron pressure. The radial location of the primary microwave heating allows phase-space holes to continue to form at larger radii. Additionally, the rf diffusion rate used in the simulation is comparable to the bounce-averaged diffusion rate [15] computed using the vacuum fields estimated from the quality of the cavity resonance. With $Q \sim 300$, the cavity electric field, E_{\perp} , is approximately 20 V/cm for 50 W.

Although the modified nonlinear simulation reproduces frequency sweeping suppression due to ECRH diffusion, some phenomena seen in the laboratory are not reproduced well by the simulation nor can the simulation properly model the long-term evolution of the plasma. For example, while frequency sweeping is arrested by apply-

ing rf fields, the HEI instability is not stabilized. Rather, it persists at a saturated level with a broadbanded spectrum that resembles the spectrum typical of the start of HEI instability bursts except at reduced amplitude and bandwidth. As expected, these chaotic modes are well-correlated with enhanced hot electron flux measured with the movable gridded particle analyzer. Additionally, frequency sweeping suppression is associated with peaking of ion saturation current profiles. Fields applied at lower frequencies, having cyclotron resonance at larger radii, create steeper gradients than when higher frequency fields are applied. These observations will be described in a separate article [22].

In summary, the first observation of the suppression of nonlinear frequency sweeping by the controlled application of low level rf fields is presented. Using a self-consistent nonlinear simulation, the frequency sweeping is understood to result from rf diffusion localized near the equatorial fundamental electron cyclotron resonance that causes the destruction of phase-space holes as predicted by a theory developed by Berk and co-workers [6].

*Electronic address: dm341@columbia.edu

- [1] T. H. O'Neil, Phys. Fluids **8**, 2255 (1965).
- [2] H. L. Berk, C. E. Nielson, and K. V. Roberts, Phys. Fluids **13**, 980 (1970).
- [3] T. M. O'Neil, J. H. Winfrey, and J. H. Malmberg, Phys. Fluids **14**, 1204 (1971).
- [4] T. H. Dupree, Phys. Fluids **15**, 334 (1972).
- [5] P. W. Terry, P. H. Diamond, and T. S. Halm, Phys. Fluids B **2**, 2048 (1990).
- [6] H. L. Berk *et al.*, Phys. Plasmas **6**, 3102 (1999).
- [7] H. L. Berk, B. N. Breizman, and M. Pekker, Phys. Plasmas **2**, 3008 (1995).
- [8] B. N. Breizman *et al.*, Phys. Plasmas **4**, 1559 (1997).
- [9] H. P. Warren and M. E. Mauel, Phys. Rev. Lett. **74**, 1351 (1995).
- [10] H. P. Warren and M. E. Mauel, Phys. Plasmas **2**, 4185 (1995).
- [11] N. A. Krall, Phys. Fluids **9**, 820 (1966).
- [12] M. E. Mauel, J. Phys. IV (France) **7**, 307 (1997).
- [13] B. Levitt, D. Maslovsky, and M. Mauel, Phys. Plasmas **9**, 2507 (2002).
- [14] D. Maslovsky, M. Mauel, and B. Levitt, IEEE Trans. Plasma Sci. **30**, 8 (2002).
- [15] M. E. Mauel, Phys. Fluids **27**, 2899 (1984).
- [16] A. Fasoli *et al.*, Phys. Rev. Lett. **81**, 5564 (1998).
- [17] A. Fasoli *et al.*, Phys. Plasmas **7**, 1816 (2000).
- [18] R. F. Heeter, A. F. Fasoli, and S. E. Sharapov, Phys. Rev. Lett. **85**, 3177 (2000).
- [19] H. P. Warren, M. E. Mauel, D. Brennan, and S. Taromina, Phys. Plasmas **3**, 2143 (1996).
- [20] H. P. Warren, A. Bhattacharjee, and M. E. Mauel, Geophys. Res. Lett. **19**, 941 (1992).
- [21] A. H. Boozer, Phys. Fluids **23**, 904 (1980).
- [22] D. Maslovsky, B. Levitt, and M. E. Mauel (to be published).